COMMUNICATION

Möbius aromatic forms of 8-π electron heteropines†

William L. Karney,*[a] Christian J. Kastrup,[b] Steven P. Oldfield[b] and Henry S. Rzepa*[b]

[a] *Department of Chemistry, University of San Francisco, California, 2130 Fulton St., San Francisco, California, 94117-1080, USA*
[b] *Department of Chemistry, Imperial College of Science, Technology and Medicine, London, UK SW7 2AY*

Received (in Cambridge, UK) 13th December 2001, Accepted 31st January 2002
First published as an Advance Article on the web 8th February 2002

Ab initio **calculations at the B3LYP//6-31G(d) level predict that Möbius-like conformations of O, NF, S and PF-substituted 7-membered ring 8-π electron perfluoroannulenes with an axis of symmetry exist, but they are of higher energy than isomers with a plane of symmetry. Chiral inversion of the Möbius perfluoroazepine system *via* a planar structure is shown to be an orbital symmetry forbidden process for a closed shell singlet state, resulting from the nodal characteristics of the highest occupied Möbius molecular orbital. The orbital origins of an unusual electron-correlation dependent lengthening predicted for the N–F bond in the Möbius conformation of the azepine but largely absent in the analogous phosphorus system are discussed. Structural variations based on incorporating a biphenyl motif are explored, but in no case was the Möbius form lower in energy than the achiral non-aromatic geometries retaining a plane of symmetry.**

Introduction

Following the inference in 1964 by Heilbronner using Hückel molecular orbital theory that a planar perimeter of p_π AOs occupied by 4*n* electrons can be twisted into Möbius form with gain of π resonance energy,[1] several carbocyclic examples of such Möbius systems have been proposed. Schleyer and coworkers were the first to suggest[2] that the charged 4*n* π-electron annulene $C_9H_9^+$ constituted a Möbius system,[2] and furthermore, using the NICS (nucleus independent chemical shift) measure of ring current[3] they demonstrated that this system displayed aromatic values consistent with Möbius aromatic character. We have most recently revealed[4] that the replacement of one or more double bonds by heteroatoms each contributing two π electrons can also demonstrate this effect, as can replacing a single alkene with an allene group. Here we report an investigation of the 7-membered ring systems containing three formal double bonds and one heteroatom as potential 4*n*-π electron Möbius-aromatic systems.

Of the four heterocyclic ring systems **1a**–**d** that we chose to investigate, variously substituted examples of all but the last have been characterised crystallographically.[5] These structures reveal that only a tub or boat shaped conformation is known, referred to here as having C_s symmetry (when symmetrically substituted). As planar species, such 4*n*-π electron rings would be formally anti-aromatic, and distortion from C_{2v} to C_s symmetry, with the accompanying bond localisation, is the normal route for reducing or eliminating anti-aromaticity. A corresponding system having some Möbius character, and with only a C_2 axis of symmetry, is another, hitherto unexplored alternative, with the potential for reversing the anti-aromaticity into aromaticity. We chose two strategies to investigate whether

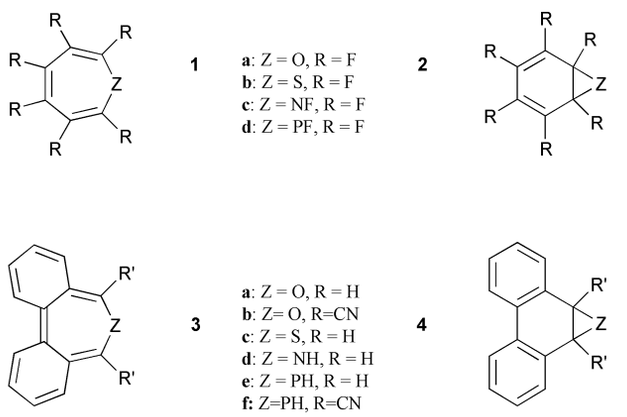

such conformations might be energetically accessible. The first involved perfluorination, which we have previously suggested[6] has the effect of reducing twist alternation in such rings and increasing aromaticity. Our second strategy was to promote C_2 symmetry and suppress C_s symmetry by constructing the 7-membered ring from the basic biphenyl motif **3**. We also included the bicyclic forms **2**, which are known to be in equilibrium with **1**, for comparison.

Computational procedure

Geometries were optimised using Gaussian 98[7] at the B3LYP/6-31G(d) level.[8] Stationary points were characterised as either minima, transition states, or higher-order saddle points by calculating the Hessian matrix and inspecting the number of negative roots and their normal mode. Nucleus-independent chemical shift (NICS) values[3] were calculated at ring centroids employing the B3LYP/6-31G(d) level of theory. Orbital plots were contoured using MacMolPlt[9] at a level of 0.02 a.u. using B3LYP/6-31G(d) wavefunctions computed with GAMESS.[10] All coordinates are available as Molfiles, together with 3D models of the orbitals expressed as 3DMF files *via* the supplemental information associated with this article.

Results and discussion

Oxepine and thiepine systems 1a and 1b

Considering firstly the perfluorooxepine **1a**, vibrational analysis of the planar system (of C_{2v} symmetry) predicts a single imaginary mode (Table) corresponding to a distortion to the lower C_s symmetry. Geometry optimization starting from a high twist C_3–C_4–C_5–C_6 dihedral angle results in *cis* to *trans* isomerism of the central formal double bond and location of a minimum with C_2 symmetry. This isomer, although 21.8 kcal mol^{-1} higher in energy than the planar C_{2v} saddle point, has an NICS value suggesting some significant aromaticity. The presence of one pseudo-*trans* component was characteristic of the $C_9H_9^+$ species identified by Schleyer[2] and has also been recently noted for cyclooctatetraene.[11] The ring bond

† Electronic supplementary information (ESI) available: all coordinates as MDL Molfiles, together with 3D models of the orbitals expressed as 3DMF files. Diagrams are also available in SVG (high resolution) format. See http://www.rsc.org/suppdata/p2/b1/b111369k/

 DOI: 10.1039/b111369k

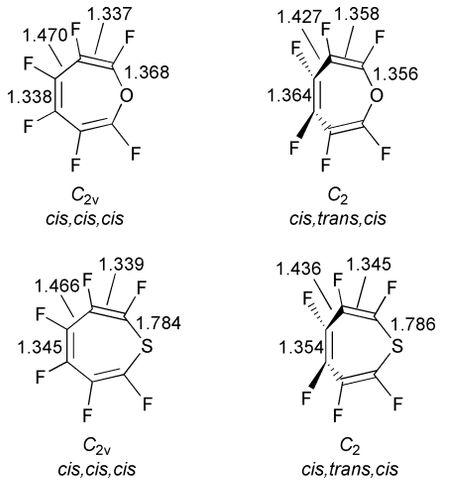

Fig. 1 B3LYP/6-31G* bond lengths (Å) for stationary points for perfluorooxepine and perfluorothiepine.

lengths of C_2-symmetric *cis,trans,cis* **1a** also reveal reduced alternation, characteristic of increased aromaticity or decreased anti-aromaticity (Fig. 1).

Two other isomers can be found for **1a**. The first results from distortion from the C_{2v} saddle point to the "tub" mode typical of 4*n* π-electron all-*cis* cyclooctatetraene and corresponds to the conformation observed in the crystal structures.[5] The second isomer, of very slightly lower energy, is the perfluorinated analogue **2a** of the known benzene oxide **2**. The C–C bond lengths of the C_2-symmetric *cis,trans,cis* isomer of thiepine **1b** indicate a slightly reduced tendency toward aromaticity for this species, compared to the oxepine (Fig. 1).

Azepine system 1c

With the nitrogen analogue, the C_{2v} geometry reveals a bond length pattern (Fig. 2) at the planar geometry which corresponds to the specific valence bond isomer **5c** (Scheme 1), one of the two possible forms resulting from a Jahn–Teller like distortion of the formally anti-aromatic 4*n* ring.

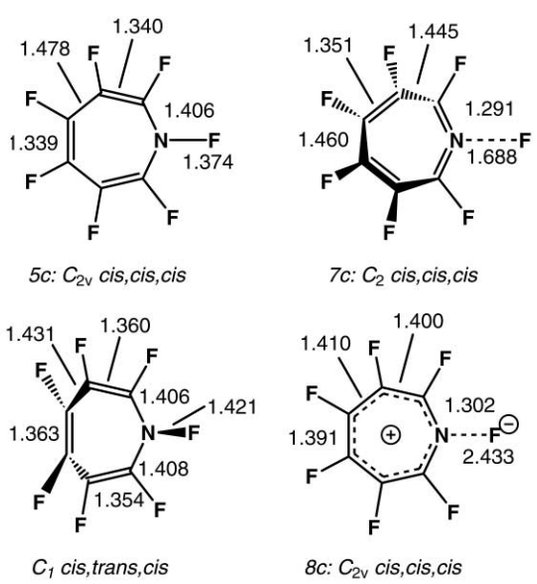

Fig. 2 B3LYP/6-31G* bond lengths (Å) for isomers of perfluoroazepine.

A high positive NICS value (17.5) confirms significant anti-aromaticity (the high value may also be due to some contamination from a smaller HOMO–LUMO energy gap). Further distortion to alleviate this anti-aromaticity is implied by the existence of two imaginary normal modes deriving from the Hessian matrix (*i.e.* this geometry is a second-order saddle point), each corresponding to C_s distortion to a lower energy form corresponding to that of the crystal structure.[5]

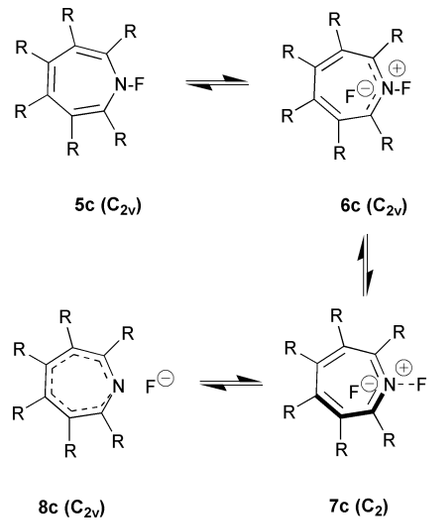

Scheme 1

Like the oxygen and sulfur systems, a C_2 symmetric form can be located which reveals an inverted NICS value indicative of moderate aromaticity. This species differs from the oxa and thia counterparts in two important ways. Firstly, the energy is lower rather than higher than at the C_{2v} geometry (by 9.2 kcal mol^{-1}). Secondly, no *trans* ring component is present, and the bond length pattern is different, corresponding more closely to that for the chiral species **7c** (Fig. 2).

Both these differences require more detailed analysis. The lower energy appears to contradict the form of the two imaginary normal modes noted above for **5c**, for which there is no C_2 symmetric distortion resulting in an energy decrease. The contradiction can be rationalised by inspecting an orbital correlation diagram between the C_{2v} (**5c**) and C_2 (**7c**) geometries (Fig. 3). This shows **5c** to have four occupied π orbitals, three of b_1 and one of a_2 symmetry. The b_1 HOMO corresponds to valence bond isomer **5c** (and the LUMO to the other possible isomer **6c**). However, **7c** has two occupied orbitals deriving from the p_π orbitals of *b* and two of *a* form. This means that the planar (anti-aromatic) Hückel isomer **5c** correlates with the doubly excited state of chiral **7c**, and *vice versa*. Such a result has indeed been previously observed for the related system cyclohepta-1,2,4,6-tetraene,[6,12] for which chiral inversion as a closed shell species is forbidden by orbital symmetry to pass through a planar form and must instead proceed through an open shell singlet state transition state.

The analogy to cycloheptatetraene also extends to the bond length pattern of **7c**, for which we note the unusually long predicted N–F bond length (Fig. 2). Before discussing this aspect in further depth in the next section, we note for completeness at this stage a further *cis,trans,cis* ring isomer of **7c** which can also be located. Rather than having C_2 symmetry, the nitrogen–fluorine axis is distorted away from the C_2 axis. This avoids destabilising repulsions between the occupied π orbital of the remote ring *trans* double bond and that of the σ N–F bonding orbital. This isomer is calculated to lie 9.8 kcal mol^{-1} above the planar stationary point **5c**, and in this relative energy and also the bond length pattern (Fig. 2), more closely resembles the results for the oxepine than for **7c**.

Origins of the unusually long N–F bond length in 7c. The remarkably long N–F bond length (1.688 Å) for **7c** compared to the value for **5c** at the planar geometry (1.374 Å) or indeed for the *cis,trans,cis* isomer (Fig. 2) requires an explanation. Firstly, we established that this value depends critically on the nature of the two atoms comprising this "single" bond. Replacing N–F with the isoelectronic C^-–F gives a normal value of 1.379 Å but equally elongated values are calculated for the other halogens (C_2/C_{2v}): N–Cl 2.463/1.719, N–Br 2.568/1.880, N–I 2.794/2.092

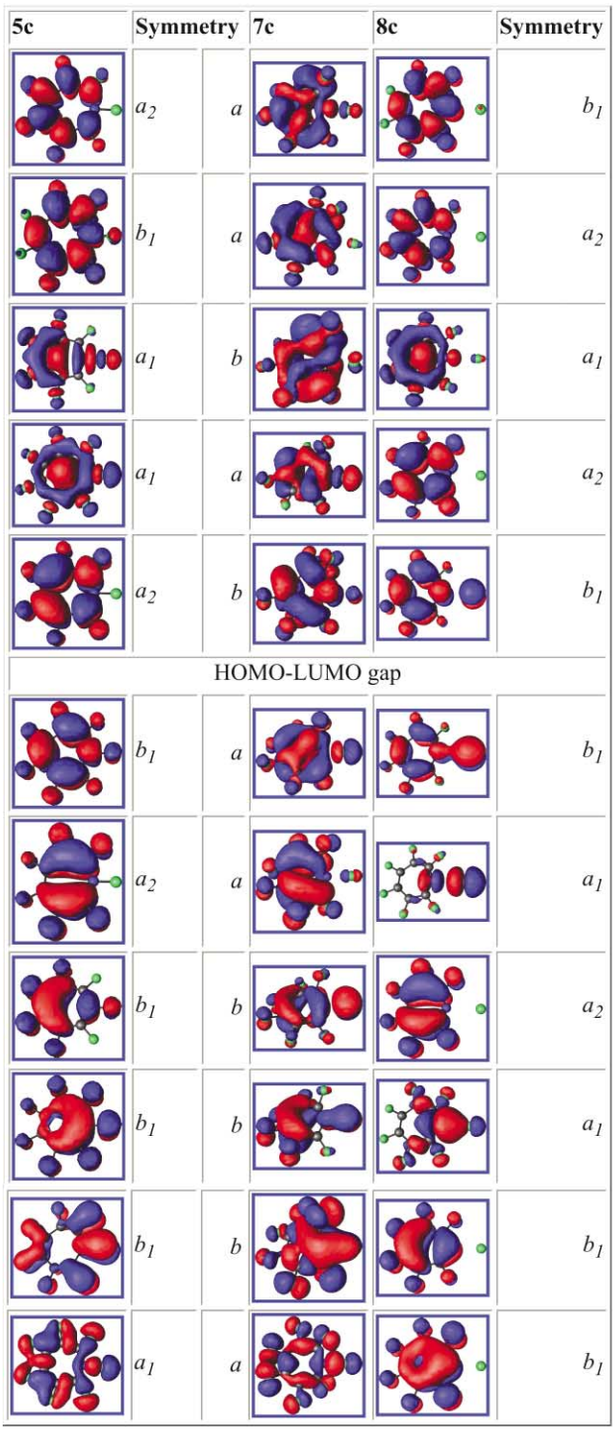

Fig. 3 B3LYP/6-31G* Orbital correlations for **5c**, **7c** and **8c**.

(at the extended B3LYP//6-311G(d) basis set level). This suggests the origins of the effect are related to the relatively low lying energy of the N–halogen σ* anti-bonding orbital, and its resulting interaction with high energy occupied orbitals of the same *a* symmetry. The effect is also dependent on the correlation treatment. At the Hartree–Fock level, the N–F bond length is almost normal (1.39 Å), but at correlated levels it is significantly lengthened (R3BYLP; 1.69, MP2; 1.70). The unusual nature of the N–halogen bond located on the C_2 axis in these systems therefore arises at least in part from a correlated interaction of the electrons in this region.

To probe this aspect further, we inspected the characteristics of the highest occupied orbital of *a* symmetry in **7c**. Qualitatively, this occupied orbital originates from the mixing induced by twisting the anti-bonding π orbital of a_2 symmetry and the anti-bonding σ orbital of a_1 symmetry in **5c**. Such mixing is of course allowed in C_2 symmetry. The effect is that one phase of the forming orbital passes directly through the C_2 axis coincident with the N–F bond, in the process establishing an anti-bonding node along this bond (Fig. 3). In this simple interpretation, the cumulative effect of creating a Möbius phase inversion by twisting the p_π system is to lengthen the N–F bond by 0.313 Å.

As we noted above, such mixing requires orbital occupancy corresponding to the doubly excited state of **5c**. The optimised planar geometry of this state (Fig. 2) corresponds closely to the representation **8c**, and its energy is 13.7 kcal mol^{-1} above that of **5c**. The vibrational analysis, unlike that of **5c** however, now does show an imaginary mode of C_2 symmetry, implying the potential energy surface is continuously connected to **7c**. This is verified by inspection of the orbital correlation (Fig. 3), which reveals how the three π and one σ orbitals of **8c** (the latter located in the N–F region) do correlate into the top four occupied orbitals of Möbius π character for **7c**. Other orbitals shown in the diagram include the HOMO of **8c** (a fluorine lone pair of b_1 symmetry) and the a_1 symmetric N–F σ bonding orbital, both of which correlate with lower lying *b* orbitals in **7c**. The overall correlation in fact is strikingly similar to that previously presented for cyclohepta-1,2,4,6-tetraene and cycloheptatrienylidene carbene.[6] To employ a more familiar metaphor, the N–F bond in this system could be described as a screw-on/screw-off type, since its length depends on the degree of twist!

Phosphepine system

Analogue **1d** shows behaviour different in several regards to that of nitrogen. A stationary point with C_{2v} symmetry was initially located with a bond length pattern corresponding to **6d** (Scheme 2, Fig. 4). The Hessian reveals it as a third order saddle

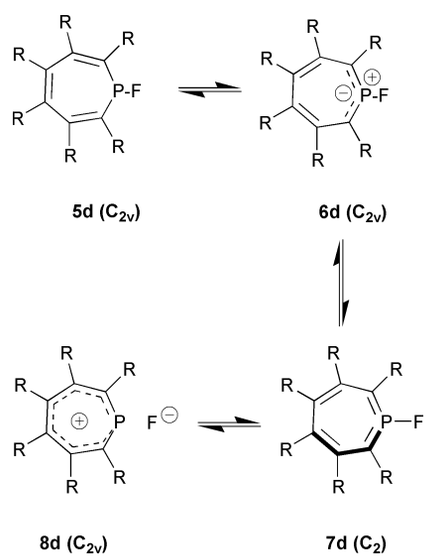

Scheme 2

point with three imaginary normal modes, the displacement vectors for the first two corresponding to C_2, and the third to C_s non-planar distortion. Appropriately, **6d** has two π orbitals of b_1 and two of a_2 symmetry, and so now correlates with the ground (rather than the excited) state of the Möbius isomer **7d** (Fig. 5), which also rationalises the presence of C_2 distortive normal modes. The NICS values again show a large inversion from anti-aromaticity to aromaticity. The difference between N and P lies in the nature of the heteroatom. With the more electronegative N, the highest occupied orbital (HOMO) has density (*i.e.* no node) on the heteroatom, whereas the less electronegative phosphorus shows no density at the HOMO.

We anticipated that, unlike the aza-analogue, a relaxed potential scan (Fig. 6) starting from the **7d** structure and incrementally reducing the C_2 twist would continuously connect to **6d**. However, the energy of the planar resulting species was 14.9 kcal mol^{-1} *lower* than **6d**, and with a structure corresponding

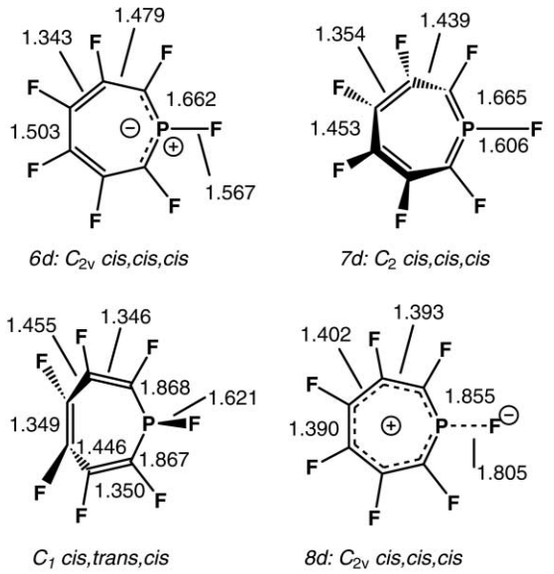

Fig. 4 B3LYP/6-31G* bond lengths (Ångstroms) for stationary points for **1d**.

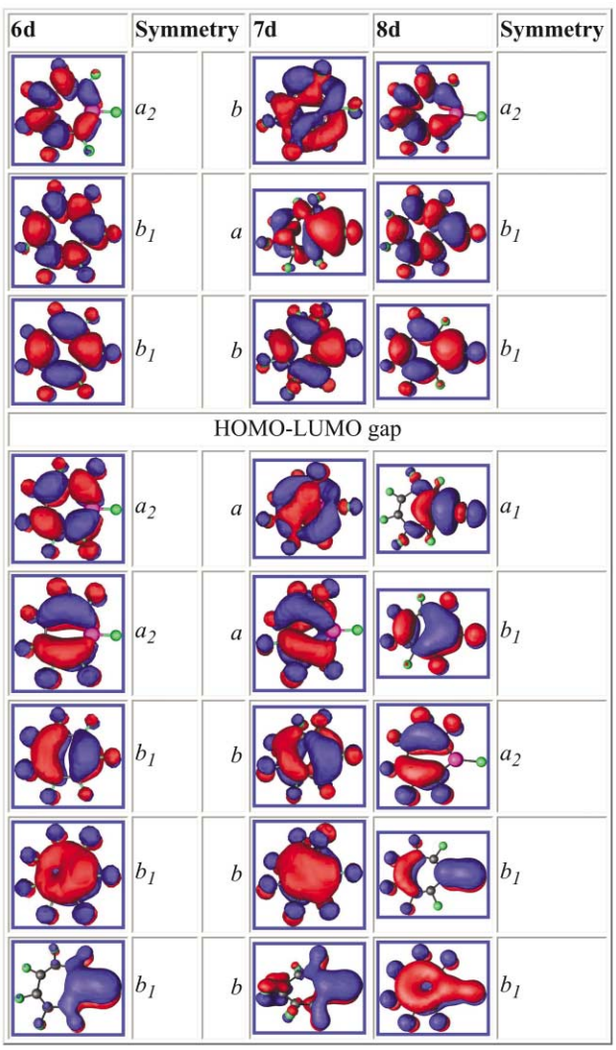

Fig. 5 B3LYP/6-31G* Orbital correlations for **6d**, **7d** and **8d**.

approximately to **8d**. Non-alternating ring bond lengths and the aromatic NICS value (−7.9 ppm) derive from some phosphatropylium fluoride ion pair character for **8d**, but the P–F bond length is much less extended than the nitrogen equivalent. An orbital correlation diagram (Fig. 5) reveals that the process of converting **7d** to **8d** again correlates only six of the eight

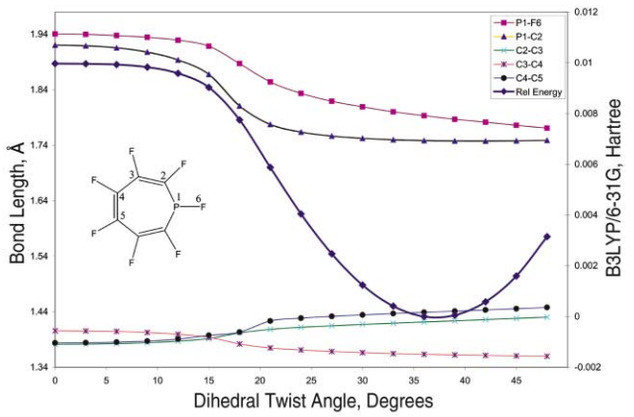

Fig. 6 A relaxed B3LYP/6-31G potential scan in C_2 symmetry connecting **7d** and **8d**. The dihedral angle is defined as C_4–Du–P–C_2, where Du is the mid-point of C_4–C_5.

ring π electrons, the remaining two converting to σ electrons occupying the P–F region, but this time in a manner which is significantly less anti-bonding along the P–F axis. Similarly, **7d** exhibits an almost normal P–F bond length, reflecting the greater degree of five-valency possible for phosphorus *via* d-orbital participation. The reduced ionic character appears associated with a greater NICS aromatic value for **7d**.

Solvation effects

Species such as **8** clearly have ionic character, and as such will be subject to greater solvation effects than the other valence isomers. To estimate the effect of solvation, we re-optimised key species using a continuum model (keyword: SCRF = DPCM) and with the default solvent water selected.

Solvation has little effect on the relative energies (Table 1); neither **7d** nor **8d** is significantly stabilised with respect to the lowest energy species of C_s symmetry, again confirming the higher hypervalency of the phosphorus centre. In contrast, the Möbius form **7c** shows extension of the N–F bond to 2.03 Å but the solvation free energy only decreases about 5 kcal mol^{-1} compared to the C_s conformation. The fully dipolar isomer **8c** reveals a decrease of about 24 kcal mol^{-1}, confirming its greater ionic characteristics. The effect of such solvation is to decrease the predicted chiral inversion barrier for **7c**.

Dibenzo substituted systems

To see if we could design a system where this energy difference might be low enough to enable experimental detection of Möbius conformations, we investigated the dibenzo derivatives. Here, the tendency to retain aromaticity in the benzo ring was designed to inhibit the C_s symmetric form, and this is indeed verified in the calculations, where no such stationary point could be located. However, ring closure to give **4** resulted in a lower energy species than the C_2 isomer **3** which was 40–53 kcal mol^{-1} higher in energy. These isomers also displayed another significant difference from the monocyclic forms. The NICS values at the 7-ring centroid indicate significant anti-aromaticity and the 6-rings are surprisingly non-aromatic. The HOMO for the aza system **3**–**10** (Fig. 7), although C_2

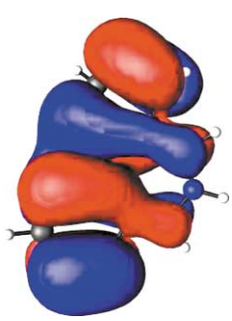

Fig. 7 B3LYP/6-31G* Highest occupied molecular orbital for **3d**.

Table 1 Energies, kcal mol^{-1}, relative to **2** or **4** (B3LYP/6-31G(d) in Hartree) and computed NICS values (ppm)

System	Point group	C=C configuration	Negative roots	Dihedral angle C_3–C_4–C_5–C_6/°	Energy relative to **2** or **4** (total energy in parentheses)	NICS(0)
1a	C_s	*cis,cis,cis*	0	0	2.6 (−902.7656)	−5.7
1a	C_2	*cis,trans,cis*	0	94.8	36.3	−10.5
1a	C_{2v}	*cis,cis,cis*	1 [a]	0.0	14.5	+9.4
1b	C_s	*cis,cis,cis*	0	0	4.7 (−1225.7418)	−8.0
1b	C_2	*cis,trans,cis*	0	107.7	36.7	−10.9
1b	C_{2v}	*cis,cis,cis*	1 [b]	0.0	21.3	+7.3
1c	C_s	*cis,cis,cis*	0	0	−21.3 {−24.7} [g] (−982.0395)	−9.5
1c	C_2	*cis,cis,cis* (**7c**)	0	32.4	4.9 {−1.1} [g]	−6.6
1c	C_1	*cis,trans,cis*	0	98.1	23.9	−10.7
1c	C_{2v}	*cis,cis,cis* (**5c**)	2 [c]	0.0	14.1	17.5
1c	C_{2v}	*cis,cis,cis* (**8c**)	2 [d]	0.0	27.8 {4.2} [g]	–
1d	C_s	*cis,cis,cis*	0	0	−11.4 {−9.8} [g] (−1268.7453)	−7.9
1d	C_2	*cis,cis,cis* (**7d**)	0	43.9	46.0 {47.7} [g]	−10.9
1d	C_1	*cis,trans,cis*	0	111.0	23.0	−6.5
1d	C_{2v}	*cis,cis,cis* (**6d**)	3 [e]	0.0	81.9	53.4
1d	C_{2v}	*cis,cis,cis* (**8d**)	3 [f]	0.0	67.0 {63.1} [g]	−8.5
3a	C_2	*cis,cis,cis*	0	39.4	40.5 (−614.7114)	26.5, −1.1 [h]
3b	C_2	*cis,cis,cis*	0	42.7	25.5 (−799.1745)	16.5, −3.1 [h]
3c	C_2	*cis,cis,cis*	0	53.8	46.2 (−937.7039)	14.9, −4.0 [h]
3d	C_2	*cis,cis,cis*	0	41.2	19.3 (−594.8438)	20.8, −1.0 [h]
3e	C_2	*cis,cis,cis*	0	58.4	52.6 (−881.4595)	8.2, −6.2 [h]
3f	C_2	*cis,cis,cis*	0	60.2	34.6 (−1065.9222)	4.0, −7.7 [h]

[a] Negative root of Hessian; 118.8i cm^{-1} corresponding to C_s distortion. [b] 89.4i cm^{-1} corresponding to C_s distortion. [c] 472.0i, 115.8i cm^{-1} corresponding to C_s distortions. [d] 59i corresponding to in-plane N–F bending and 54i cm^{-1} corresponding to C_2 distortion. [e] 382.7i and 119.3i cm^{-1} corresponding to C_2 distortions and 270.9i corresponding to C_s distortion. [f] 495.3i cm^{-1} (b_1) corresponding to C_s distortion, 205.4i cm^{-1} (b_2) corresponding to in-plane P–F bending and 62.8i cm^{-1} (a_2) corresponding to C_2 distortion. [g] SCRF(DPCM) Solvation model. [h] Value for 6-ring.

symmetric, is quantitatively different from that for **7c** (Fig. 3) in having little density at the ring centroid. Replacing R = H by R = CN (which promotes the dipolar resonance form **10**, Scheme 3) enhances the Möbius characteristics, but insufficiently to render this the most stable form.

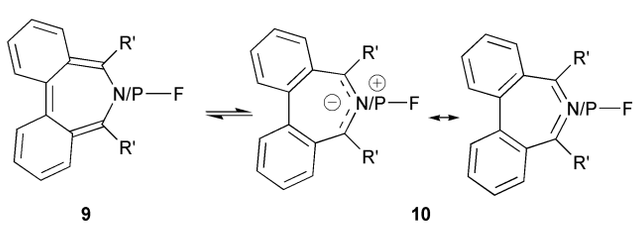

9 **10**

Scheme 3

Conclusions

The calculations reported here indicate that Möbius forms of the 8-π electron 7-membered ring analogues of the aromatic 5-membered heterocycles are minima in their respective potential surfaces, and reveal aromatic properties. Their energies, however, preclude likely experimental detection. The Möbius form of the azepine does induce an unusual example of electron correlation and electronegativity dependence in a specific bond length, the relevant bond lying along the C_2 symmetry axis and hence intercepting the Möbius π density. Suppressing the low energy non-aromatic C_s Hückel form with a potentially chiral biphenyl motif promotes the formation of the bicyclic isomers rather than the higher energy C_2 symmetric isomers, and the central 7-ring retains anti-aromatic character.

Acknowledgements

WLK is grateful to the University of San Francisco Faculty Development Fund and the Lily Drake Cancer Research Fund for generous financial support.

References

1 E. Heilbronner, *Tetrahedron Lett.*, 1964, **5**, 1923.
2 M. Mauksch, V. Gogonea, H. Jiao and P. v. R. Schleyer, *Angew. Chem., Int. Ed.*, 1998, **37**, 2395.
3 For references to the NICS technique, see P. v. R. Schleyer, C. Maerker, A. Dransfeld, H. Jiao and N. J. R. van Eikema Hommes, *J. Am. Chem. Soc.*, 1996, **118**, 6317; H. Jiao and P. v. R. Schleyer, *J. Phys. Org. Chem.*, 1998, **11**, 655.
4 C. Kastrup, S. Oldfield and H. S. Rzepa, *Chem. Commun.*, 2001 (DOI: 10.1039/b110626k).
5 (*a*) 2,7-Diphenyloxepine: M. J. McManus, G. A. Berchtold, D. R. Boyd, D. A. Kennedy and J. F. Malone, *J. Org. Chem.*, 1986, **51**, 2784; (*b*) 1-(4-Bromophenylsulfonyl)-1*H*-azepine: I. C. Paul, S. M. Johnson, L. A. Paquette, J. H. Barrett and R. J. Haluska, *J. Am. Chem. Soc.*, 1968, **90**, 5023; (*c*) 2,7-Di-*tert*-butylthiepine: K. Yamamoto, S. Yamazaki, Y. Kohashi, I. Murata, Y. Kai, N. Kanehisa, K. Miki and N. Kasai, *Tetrahedron Lett.*, 1982, **23**, 3195; (*d*) No X-ray structures of phosphepines have been reported, but a synthesis is available: G. Keglevich, *Synthesis*, 1993, 931–942.
6 S. Martin-Santamaria and H. S. Rzepa, *Chem. Commun.*, 2000, 1089; S. Martin-Santamaria and H. S. Rzepa, *J. Chem. Soc., Perkin Trans. 2*, 2000, 2372–2377.
7 Gaussian 98 (Revision A.8), M. J. Frisch, G. W. Trucks, H. B. Schlegel, G. E. Scuseria, M. A. Robb, J. R. Cheeseman, V. G. Zakrzewski, J. A. Montgomery, Jr., R. E. Stratmann, J. C. Burant, S. Dapprich, J. M. Millam, A. D. Daniels, K. N. Kudin, M. C. Strain, O. Farkas, J. Tomasi, V. Barone, M. Cossi, R. Cammi, B. Mennucci, C. Pomelli, C. Adamo, S. Clifford, J. Ochterski, G. A. Petersson, P. Y. Ayala, Q. Cui, K. Morokuma, D. K. Malick, A. D. Rabuck, K. Raghavachari, J. B. Foresman, J. Cioslowski, J. V. Ortiz, A. G. Baboul, B. B. Stefanov, G. Liu, A. Liashenko, P. Piskorz, I. Komaromi, R. Gomperts, R. L. Martin, D. J. Fox, T. Keith, M. A. Al-Laham, C. Y. Peng, A. Nanayakkara, C. Gonzalez, M. Challacombe, P. M. W. Gill, B. G. Johnson, W. Chen, M. W. Wong, J. L. Andres, M. Head-Gordon, E. S. Replogle and J. A. Pople, Gaussian, Inc., Pittsburgh PA, 1998 .
8 B3LYP method: A. D. Becke, *J. Chem. Phys.*, 1993, **98**, 5648; C. Lee, W. Yang and R. G. Parr, *Phys. Rev. B*, 1988, **37**, 785; 6-31G* basis set: P. C. Hariharan and J. A. Pople, *Theor. Chim. Acta*, 1973, **28**, 213.
9 B. M. Bode and M. S. Gordon, *J. Mol. Graphics Modell.*, 1999, **16**, 133–138.
10 M. W. Schmidt, K. K. Baldridge, J. A. Boatz, S. T. Elbert, M. S. Gorgon, J. H. Jensen, S. Koseki, N. Matsunaga, K. A. Nguyen, S. J. Su, T. L. Windus, M. Dupuis and J. A. Montgomery, *J. Comput. Chem.*, 1993, **14**, 1347–1363.
11 R. P. Johnson and K. J. Daoust, *J. Am. Chem. Soc.*, 1996, **118**, 7381–7385; R. W. A. Havenith, J. H. Van Lenthe and L. W. Jenneskens, *Int. J. Quantum Chem.*, 2001, **85**, 52–60.
12 P. R. Schreiner, W. L. Karney, P. v. R. Schleyer, W. T. Borden, T. B. Hamilton and H. F. Schaefer, *J. Org. Chem.*, 1996, **61**, 7030–7039; W. L. Karney and W. T. Borden, *J. Am. Chem. Soc.*, 1997, **119**, 1378–1387.